

Design and Analysis of 5-DOF Micro/nano-Positioning Stage

Chao Lin

The State Key Laboratory of Mechanical Transmission, Chongqing University,
Chongqing, China
Email: linchao@cqu.edu.cn

Xinhui Cui, Kai Cheng and Songsong Yu

The State Key Laboratory of Mechanical Transmission, Chongqing University,
Chongqing, China
Email: {cuixinhui0207, chengkai, yuss0417}@163.com

Abstract—This paper provided a design method for configuration synthesis of micro/nano-positioning stage with bridge-type mechanism based on graph theory. The structural characteristics of stage were discussed first. Then, these modules made up of micro/nano-positioning stage were abstracted. Thus the stage could be described with a tree-graph. According to the spanning tree theory, several possible configurations of stage were enumerated correspondingly. Subsequently, the configuration synthesis of six bridge-type mechanisms was investigated and 720 results were obtained. Rules for generating structures with symmetry were established. On the basis of this, several innovative structures were presented, and one example was chosen for further analysis. The performance of the selected stage was confirmed by finite element analysis (FEA), and a prototype of the selected stage was fabricated for performance tests. Both FEA simulation and experimental studies well validate the performance of the selected stage that is expected to be adopted in micro/nano-positioning stage. Furthermore, the result of this paper provides a practicable approach for the structural design of stage and the design method based on graph theory is effective.

Index Terms—Micropositioning, Nanopositioning, Bridge-type mechanism, Finite element analysis, Graph theory, Design method.

I. INTRODUCTION

Nowadays, with the development of precision engineering, micro/nano-positioning stage driven by stack type piezoelectric elements plays a very important role in modern technology. During the past two decades considerable research has been conducted to develop micro/nano-positioning stage to be used for purposes such as biological cell manipulation in biotechnology [1], micro-component assembly in micro-technology [2],

scanning probe microscope [3], and single-step nano-imprint lithography [4]. Whereas, the design methods of micro/nano-positioning stage are mostly from the designers' inspiration, and the design about stage with multi-DOFs is always difficult. Choi et al. [5] proposed a novel piezo-driven compliant stage for long travel range with nano-motion. Li et al. [6] provided a totally decoupled flexure-based XY parallel micromanipulator with both input and output decoupling. Despite several XY stage designs that exist in the literature [7-8], achieving multi-DOFs for the stage has been a challenge. In recent research, $XY\theta_z$, XYZ, $Z\theta_x\theta_y$ and 6-DOF stages have been developed. Yi et al. [9], Lu et al. [10] and Chang et al. [11] focused studies on $XY\theta_z$ -stages. In some applications, such as optical alignment, XYZ-stage is required. Xu et al. [12] presented a design procedure for a new decoupled flexure-based XYZ compliant parallel-kinematics micropositioning stage and designed an XYZ-stage owned a compact structure constructed by three monolithic limbs and has both input and output decoupling properties. Zhang et al. [13] developed a novel three degree of freedom numerically controlled micro-positioning table for applications such as improving the machining precision of precision grinders. Cheng et al. [14] developed a 6-DOF monolithic nanopositioning stage for three coordinate measuring machine (CMM) with nanometer resolution. Liang et al. [15] described the design of a micro-scale manipulator based on a six-DOF compliant parallel mechanism (CPM) with integrated force sensor.

In the past few years, many researchers had devoted to finding a systematic approach to design all possible structures. The pseudo-rigid-body model (PRBM) approach was firstly put forward by Howell [16], which was widely used in analysis of compliant mechanisms, despite its inadequacy in the structural design. A Freedom and Constraint Topology (FACT) approach, which is based on screw theory and founded on constraint-based design theory, was proposed by Hopkins et al. [17] to aid the conceptual design of compliant mechanisms. Yu et al. [18] provided a systematic formulation of the type synthesis of parallel, serial, and hybrid flexure systems

This research was supported by the State Key Laboratory of Mechanical Transmission (No. 0301002109150) and a grant from research foundation of the State Key Laboratory of Mechanical Transmission (2009).

Corresponding author: cuixinhui0207@163.com

via a mapping from a geometric concept to physical entity. The whole type synthesis principle was built upon screw system theory and the modified FACT approach. So far, more and more researchers have set out to study on the systematic approach.

Graph theory is an emerging branch of mathematics, which is mainly used to study a collection of vertices or nodes and a collection of edges that connect pairs of vertices. It plays a very significant role in the structural design of mechanism. The design with the aid of graph theory is simply and quickly. Lin et al. [19] studied the structural synthesis of compliant translational mechanisms (CT mechanisms) with the aid of graph theory. Yan et al. [20] provided an algorithm, based on graph theory, for enumerating all feasible serial and/or parallel combined mechanisms from the given rotary or translational power source and specific kinematic building blocks. Yu et al. [21] put forward a simple but effective configuration synthesis method for reconfigurable robot based on the graph theory. The algorithm put forward by Yan et al. [20] was modified and employed in this paper.

In the remainder of the paper, the design and enumeration of micro/nano-positioning stage are presented in Section II, where a 5-DOF positioning stage is proposed as an example for the subsequent studies. The performance of the 5-DOF positioning stage was confirmed by finite element analysis (FEA) in Section III. Moreover, the stage is fabricated along with experiments conducted in Section IV. Finally, some concluding remarks are summarized in Section V.

II. DESIGN AND ENUMERATION OF MICRO/NANO-POSITIONING STAGE

A. The Process of Configuration Synthesis

Micro/nano-positioning stage commonly employs piezoelectric actuators (PZT) which is known for the unique features of compact size, swift response, high resolution, electrical mechanical coupling efficiency, and low heat and flexure hinges which have negligible stick-slip, continuous displacement, negligible backlash, no need for lubrication, and high precision [22]. Although piezoelectric actuators can provide a larger output force, they have a limited deformation range of about 10µm/cm. The small displacement is not sufficient for most general engineering applications, thus the amplifying mechanism is necessary in the micro/nano-positioning stage. According to the amplify theory, the displacement-amplification mechanisms can be divided into four classes: the lever-type mechanism, the bridge-type mechanism [23], the eight-bar mechanism and the Scott-Russel mechanism [24], as shown in TABLE I. Thus, micro/nano-positioning stage can be transformed into the graph consisting of a collection of vertices and a collection of edges that connect pairs of vertices, where vertices denote modules and edges denote the relationship between them.

TABLE I. CLASSIFICATION OF DISPLACEMENT-AMPLIFICATION MECHANISMS

Classification	Topology	Motion function	Simplified representation
Lever-type mechanism		translation-rotation	(T, R)
Bridge-type mechanism		translation-translation	(T, T)
Eight-bar mechanism		translation-translation	(T, T)
Scott-Russel mechanism		translation-translation	(T, T)

Select the appropriate modules based on design requirements: Select the appropriate modules to prepare for the design. One or two class module can be selected for the micro/nano-positioning stage, which is characteristic of compact structure. However, in order to obtain multi-DOFs for the stage, the number of each module can be selected more. The modules are identified as single-input and single-output mechanisms. Thus, the input/output links can be represented as (J_{input} , J_{output}) for every module. Then, their possible representations of input-output joint types are listed in TABLE I.

The bridge-type amplification mechanism has a compact structure and a large displacement amplification ratio. Two bridge-type mechanisms are selected in the introduction of the approach.

Generate the connected digraph: The connected digraph called path-digraph represents all possible paths of motion transmission among these modules. The path-digraph, D, as shown in Fig. 1, can be generated by representing the numbered modules and the stage as labeled vertices, and using the directed edges to describe all the feasible combination relationships between any two vertices that could be combined. In the path-digraph, the stage is represented as the vertice M, and the direction of each edge indicates the direction of motion transmission. In order to avoid repetitive spanning tree when the selected modules belong to one class, the directed edges between any two numbered vertices can be reduced to only one. As shown in Fig. 2.

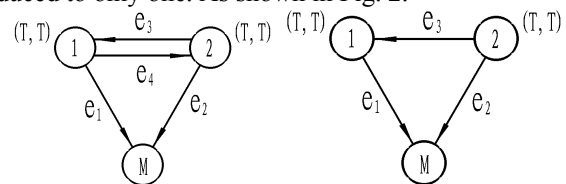


Figure 1. Path-digraph D Figure 2. Simplified path-digraph D_s

Enumerate all spanning trees of the path-digraph: Enumerate all spanning trees of the path-digraph by adopting the algorithm of tree enumeration in graph theory [25]. Two mathematical forms, edge permutation

sequence (EPS) and path-incidence matrix, are applied to capture the information of all directed edges in the path-digraph [20]. The edge permutation sequences for the simplified path-digraph D_s is presented as:

$$E = (e_1 e_2 e_3) = \begin{bmatrix} V_1 & V_2 & V_2 \\ M & M & V_1 \end{bmatrix} \quad (1)$$

where e_i represents the i^{th} directed edge in the simplified path-digraph D_s , the first row lists every starting point of the corresponding directed edge, and the second row lists every end point of the corresponding directed edge.

According to the principle of the path-incidence matrix in graph theory, the corresponding path-incidence matrix of the simplified path-digraph D_s is:

$$B = \begin{matrix} & e_1 & e_2 & e_3 \\ M & \begin{bmatrix} -1 & -1 & 0 \\ 1 & 0 & -1 \\ 0 & 1 & 1 \end{bmatrix} \end{matrix} \quad (2)$$

For a path-digraph, let B_R (reduced incidence matrix) be its path-incidence matrix B with the row corresponding the vertex 'M' removed, and let \bar{B}_R be a matrix (nonnegative reduced incidence matrix) by changing all elements of -1 in B_R to 0. Then, the reduced incidence matrix B and nonnegative reduced incidence matrix \bar{B}_R can be obtained as follow:

$$B_R = \begin{matrix} & e_1 & e_2 & e_3 \\ V_1 & \begin{bmatrix} 1 & 0 & -1 \\ 0 & 1 & 1 \end{bmatrix} \\ V_2 & \end{matrix} \quad (3)$$

$$\bar{B}_R = \begin{matrix} & e_1 & e_2 & e_3 \\ V_1 & \begin{bmatrix} 1 & 0 & 0 \\ 0 & 1 & 1 \end{bmatrix} \\ V_2 & \end{matrix} \quad (4)$$

According to the formula of spanning tree in graph theory, the possible spanning graphs can be generated by expanding the determinant of product matrix $\bar{B}_R \cdot \bar{B}_R^T$. The product matrix $\bar{B}_R \cdot \bar{B}_R^T$ is a diagonal matrix and the value of each non-zero element can be explained as the number of directed edges from each vertex to others except the vertex M. Thus, the number in the product matrix can be substituted for the addition of corresponding directed edges. Therefore, the expansions of the determinant of $\bar{B}_R \cdot \bar{B}_R^T$ can be obtained as:

$$\det(\bar{B}_R \cdot \bar{B}_R^T) = \det \begin{bmatrix} 1 & 0 \\ 0 & 2 \end{bmatrix} \Rightarrow \begin{vmatrix} e_1 & 0 \\ 0 & e_2 + e_3 \end{vmatrix} = e_1 e_2 + e_1 e_3 \quad (5)$$

Each term in (5) donates a spanning tree of the simplified path-digraph D_s in Fig. 2 and the corresponding spanning graphs can be drawn according to the edge permutation sequence in (1). Thus, a feasible stage should be represented as a spanning in-tree with the stage as the endpoint. Subsequently, all feasible spanning

graphs can be obtained based on the principle, as shown in Fig. 3.

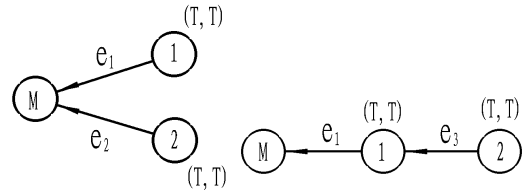


Figure 3. All feasible spanning graphs

Concretize every spanning in-tree: All possible configurations of stage can be obtained by concretizing every spanning in-tree. The method of concretization is to transform the vertices to the corresponding stage and modules, and combine them by following the directions of motion transmission in the simplified path-digraph D_s . In this way, two feasible micro/nano-positioning stages can be obtained, as shown in Fig. 4.



Figure 4. Two feasible micro/nano-positioning stages

B. Configuration synthesis of micro/nano-positioning stage with multi-DOFs.

The approach presented in the previous section will be applied to the configuration of stage with multi-DOFs. To obtain multi-DOFs, six bridge-type mechanisms will be selected, because the bridge-type mechanism has a compact structure and a large displacement amplification ratio. According to the proposed simplified principle, the simplified path-digraph D_1 can be generated, as shown in Fig. 5.

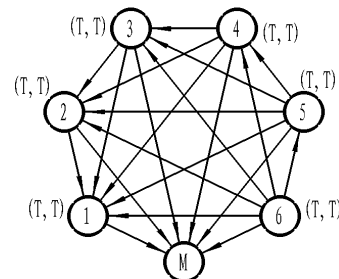


Figure 5. Simplified path-digraph D_1

The edge permutation sequence for the simplified path-digraph D_1 is presented as:

$$E = (e_1 e_2 e_3 e_4 e_5 e_6 e_7 e_8 e_9 e_{10} e_{11} e_{12} e_{13} e_{14} e_{15} e_{16} e_{17} e_{18} e_{19} e_{20} e_{21}) \quad (6)$$

$$= \begin{bmatrix} V_1 & V_2 & V_3 & V_4 & V_5 & V_6 & V_2 & V_3 & V_4 & V_5 & V_6 & V_3 & V_4 & V_5 & V_6 & V_4 & V_5 & V_6 & V_3 & V_6 & V_6 \\ MMMMMM & V_1 & V_1 & V_1 & V_1 & V_2 & V_2 & V_2 & V_2 & V_3 & V_3 & V_3 & V_4 & V_4 & V_5 \end{bmatrix}$$

According to the method mentioned above, B , B_R and \bar{B}_R of the simplified path-digraph D_1 can be obtained in turn. Thus, B can be obtained in (7), and the expansion of the determinant of $\bar{B}_R \cdot \bar{B}_R^T$ can be obtained as:

3	$e_1e_2e_3e_4e_{10}e_{15}$ $e_1e_2e_3e_4e_{10}e_{20}$ $e_1e_2e_3e_4e_{10}e_{18}$			5
	$e_1e_2e_3e_4e_{10}e_{18}$			4
4	$e_1e_2e_3e_4e_5e_6$			4

III. PERFORMANCE EVALUATION WITH FEA

To overcome the coupled motion between the outputs, the motion guide mechanism with flexures is essential in the stage. Finally, the schematic drawing and the model of the 5-DOF monolithic nanopositioning stage are shown in Fig. 7 and Fig. 8, respectively.

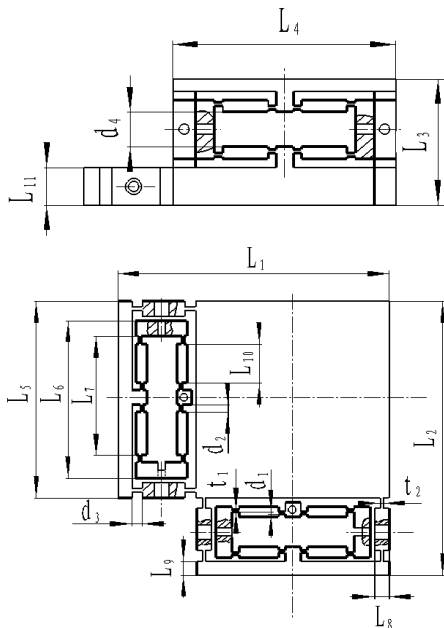


Figure 7. The schematic drawing of the 5-DOF monolithic nanopositioning stage

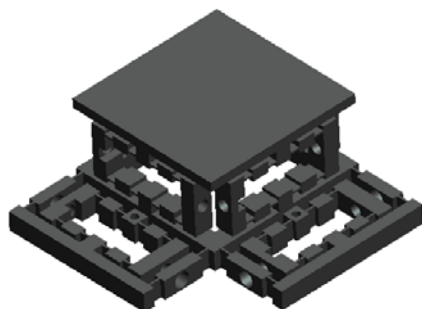
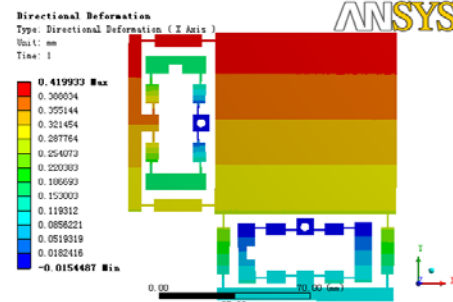


Figure 8. The model of the 5-DOF monolithic nanopositioning stage

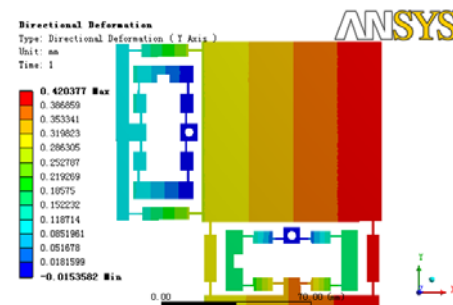
The performance of the stage is verified by the FEA with ANSYS software package. The material selected is the spring steel (65Mn), and the material parameters are shown in TABLE IV. As shown in Fig. 7, the dimensions for the improved stage (No.2) are as follow: Total length (L_1) and width (L_2) for the stage are both 122mm, height (L_3) is 50mm. The up platform is a square, the length (L_4) of which is 82mm, as is L_5 . Length for the bridge-type mechanism $L_6=62$ mm, $L_7=46$ mm, $L_{10}=9$ mm, $L_{11}=13$ mm, and Length for the motion guide mechanism with flexures $L_8=6$ mm, $L_9=6$ mm. The dimensions for the beam hinge are as follow: $d_1=1$ mm, $d_2=5$ mm, $d_3=6$ mm, $d_4=16$ mm. The crucial dimension t_1 and t_2 are both 1mm. In addition, the PZT (40VS15) has a length of 46mm, which can produce the maximal travel range of 40 μ m and the maximal output force of 900N.

TABLE IV. MATERIAL PARAMETERS

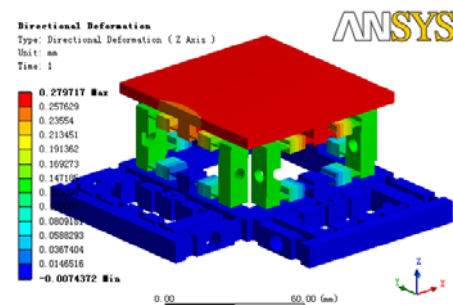
Young's modulus	Yield strength	Material density	Poisson's ratio
210GPa	780 MPa	7850 kg·m ⁻³	0.3



(A) Along the x-axis



(B) Along the y-axis



(C) Along the z-axis

Figure 9. Static structural FEA results of deformations along the three axes of the 5-DOF stage

When a displacement (0.02mm) is applied at the two input ends of the bridge-type mechanism, a static structural analysis along the x-axis is carried out and the stage deformation is depicted in Fig. 9. With the same method, the maximal displacement along the X-, Y-, and Z-axis are 434 μ m, 435 μ m and 286 μ m. When the 5-DOF stage reaches the maximum displacement along the X-, Y- and Z-axis, the maximum stress occurring at the beam hinge point are 392.57Mpa, 394.99Mpa and 393.27Mpa, respectively. These are all quite smaller than the yield strength of 780Mpa (65Mn), as shown in TABLE V.

TABLE V.
FINITE ELEMENT ANALYSIS RESULTS

	X-axis	Y-axis	Z-axis
Maximum displacement(μ m)	434	435	286
Maximum stress(Mpa)	392.57	394.99	393.27

IV. EXPERIMENTAL RESULTS AND DISCUSSIONS

In order to verify the maximal displacement of stage, experimental system are set up shown in Fig.10, which consists of PZT (Pst 40VS15), PZT controller and laser sensor. The PZT achieves input resolution at 0.8nm, along with maximum stroke at 40 μ m under closed-loop control.

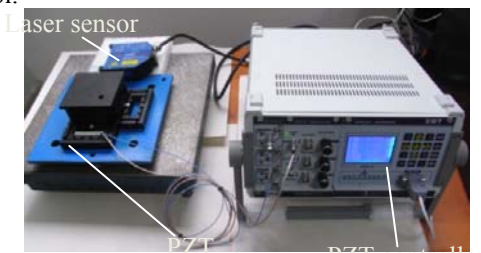


Figure 10. Experimental testing system

Taking the output along x-axis as an example, when the PZT input displacement increase, output is detected by the laser sensor ILD1700 (MICRO-EPSILON) with resolution of 0.25 μ m and measuring range 10mm. The experimental result and ANSYS simulation result are shown in Fig. 11. The maximum travel along the x-axis is 354 μ m. The results are shown in TABLE VI.

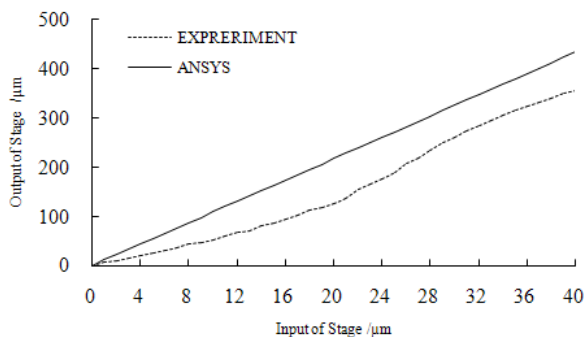


Figure 11. The experimental result and ANSYS simulation result

Compared with the ANSYS simulation result, the experimental result is less than that. There are two reasons, one is that PZT stiffness is neglected in the ANSYS simulation, and the other is mainly stemmed

from the change of material property caused by high-temperature of wire cutting.

TABLE VI.
FINITE ELEMENT ANALYSIS AND EXPERIMENTAL RESULTS

Input (μ m)	X-axis(μ m)		Y-axis(μ m)		Z-axis(μ m)	
	Ansys	Exp.	Ansys	Exp.	Ansys	Exp.
4	43.5	22.5	42.4	20.6	28.5	-
8	86.8	48.7	85.6	44.7	57.6	-
12	130.6	70.8	129.7	66.7	85.8	-
16	173.6	95.4	171.9	93.9	114.5	-
20	217.3	118.5	216.8	116.6	142.9	-
24	260.5	168.3	258.9	165.9	171.4	-
28	303.8	220.3	302.5	218.3	200.3	-
32	347.2	268.6	348.5	265.6	228.6	-
36	390.6	305.3	307.2	304.9	257.1	-
40	434	354.4	435	352.8	286	-

V. CONCLUSIONS

In summary, this paper presented a feasible approach based on graph theory to obtain several possible configurations of micro/nano-positioning stage with bridge-type amplification mechanism. By this method, several innovative structures with multi-DOFs could be obtained exactly and directly. The performance of a newly 5-DOF positioning stage was confirmed by FEA and experimental studies, which show that the newly 5-DOF stage has a larger displacement output and has a compact structure.

Although bridge-type mechanism was only selected in this paper, this method was also applicable for other amplifying mechanisms in the configuration of micro/nano-positioning stage. The result of this paper demonstrates that this method is effective for the structural design of stage. Meanwhile, the design method with the aid of graph theory is simple and quick.

ACKNOWLEDGMENT

It is a key project supported by the State Key Laboratory of Mechanical Transmission (No. 0301002109150) and a grant from research foundation of State Key Laboratory of Mechanical Transmission (2009).

REFERENCES

- [1] T. Ando, N. Kodera, D. Maruyama, E. Takai, K. Saito, and A. Toda, "A high-speed atomic force microscope for studying biological macromolecules in action," *Japanese Journal of Applied Physics*, vol. 41, pp. 4851-4856, 2002.
- [2] M. L. Culpepper and G. Anderson, "Design of a low-cost nano-manipulator which utilizes a monolithic, spatial compliant mechanism," *Precision Engineering*, vol. 28(4), pp. 469-482, 2004.
- [3] R. Yang, M. Jouaneh, and R. Schweizer, "Design and characterization of a low-profile micropositioning stage," *Precision Engineering*, vol.18, pp. 20-29, 1996.
- [4] K. B. Choi and J. J. Lee, "Passive compliant wafer stage for single-step nano-imprint lithography," *Review of scientific instruments*, vol.76, pp.1-6, 2005.
- [5] K. B. Choi, J. J. Lee, and S. H. "A piezo-driven compliant stage with double mechanical amplification mechanisms

- arranged in parallel,” *Sensors and Actuators*, vol.A161, pp.173–181, 2010.
- [6] Y. M. Li and Q.S. Xu. “Design and analysis of a totally decoupled flexure-based XY parallel micromanipulator,” *Transactions on Robotics*, vol. 25, pp.645–657, June 2009.
- [7] Y.M. Li and Q.S. Xu, “Development and assessment of a novel decoupled XY Parallel Micropositioning Platform.” *IEEE/ASME Transactions on Mechatronics*, Vol. 15, pp.125–135, February 2010.
- [8] Y. K. Yong, S. S. Aphale, and S. O. Reza Moheimani, “Design, identification, and control of a flexure-based XY stage for fast nanoscale positioning.” *IEEE Transactions on Nanotechnology*, Vol. 8, pp. 46–54, January 2009.
- [9] B. J. Yi, G. B. Chung, H. Y. Na, W. K. Kim, and I. H. Suh, “Design and experiment of a 3-DOF parallel micromechanism utilizing flexure hinges.” vol.19, pp. 604–611, August 2003.
- [10] Y. K. Yong and T. F. Lu. “Kinetostatic modeling of 3-RRR compliant micro-motion stages with flexure hinges.” vol.44, pp.1156–1175, 2009.
- [11] S. H. Chang, C. K. Tseng, and H. C. Chien, “An ultra-precision XY θ_z piezo-micropositioner part I: design and analysis.” *IEEE Transactions on Ultrasonics, Ferroelectrics, and Frequency Control*, vol. 46, pp.897–904, July 1999.
- [12] Q.S. Xu and Y.M. Li. “Design of a new decoupled XYZ compliant parallel micropositioning stage with compact structure.” *Proceedings of the 2009 IEEE International Conference on Robotics and Biomimetics* December 19–23, 2009, Guilin, China
- [13] D. Zhang, D.G. Chetwyndb, X. Liu, and Y. Tian. “Investigation of a 3-DOF micro-positioning table for surface grinding.” *International Journal of Mechanical Sciences*, vol.48 pp.1401–1408, 2006.
- [14] L.L. Cheng, J.W. Yu, and X.F. Yu. “Design and analysis of a 6-DOF monolithic nanopositioning stage.” *Key Engineering Materials*, vol.437, pp.61–65. May 2010.
- [15] Q. K. Liang, D. Zhang, Z. Z. Chi, Q. J. Song, Y. J. Ge, and Y. G. “Six-DOF micro-manipulator based on compliant parallel mechanism with integrated force sensor.” *Robotics and Computer-Integrated Manufacturing*, vol.27, pp.124–134, 2011.
- [16] L. L. Howell *Compliant mechanisms*. New York: Wiley Interscience, 2001.
- [17] J. B. Hopkins and M. L. Culpepper, “Synthesis of multi-degree of freedom, parallel flexure system concepts via freedom and constraint topology (FACT). Part I: principles.” *Precision Engineering*, vol. 34, pp. 259–270, 2010.
- [18] J. J. Yu, S.Z. Li, and X. Pei, “Type synthesis principle and practice of flexure systems in the framework of screw theory part I: General methodology.” *2010 ASME International Design Engineering Conference*, New York: ASME, 2010: DETC2010–28783.
- [19] Y.T. Lin and J.J. Lee, “Structural synthesis of compliant translational mechanisms.” 12th IFToMM World Congress, June 18–21, 2007, Besançon, France.
- [20] H. S. Yan, F. M. Ou and M. F. Tang. “An algorithm for the enumeration of serial and/or parallel combinations of kinematic building blocks.” *In Proceedings of DETC’04*, Salt Lake City, Utah, DETC2004–57295.
- [21] H. B. Yu, J. J. Yu, S. S. Bi, and G. H. Zong, “Configuration synthesis of reconfigurable robot based on graph theory.” vol. 4, pp.79–83, Aug 2005.
- [22] W.Y. Jywe, Y.R. Jeng, and C.H. Liu, “A novel 5 DOF thin coplanar nanometer-scale stage.” *Precision Engineering*. vol.32, pp. 239–250, November 2008.

- [23] H.W. Ma, S.M. Yao, L.Q. Wang, and Z. Zhong, “Analysis of the displacement amplification ratio of bridge-type flexure hinge.” *Sensors and Actuators* vol.A 132, pp.730–736, 2006.
- [24] Y.L. Tian, B.J. Shirinzadeh, D.W. Zhang, and GurselAlici, “Development and dynamic modelling of a flexure-based Scott–Russell mechanism for nano-manipulation.” *Mechanical Systems and Signal Processing*, vol.23, pp. 957–978, 2009.
- [25] K.C. Lu and H.M. Lu. *Graph theory and applications (Second Edition)*. Tsinghua University Press, 1995.



Chao Lin received the B.E. degree in machine manufacturing and equipments automate, M.E. degree in mechanics and Ph.D. degree in mechanical design and theory from Chongqing University, Chongqing, China, in 1988, 1996 and 2002, respectively.

He is currently a Professor of mechanical design and theory at the University of Chongqing, Chongqing, China, where he also undertake the teaching course that the graduate course 10 and undergraduate course 4. He has authored or coauthored more than 50 scientific papers. His current research interests in micro/nano-transmission platform and the transmission theory.

Prof. Lin is an advanced member of Chinese Journal of Mechanical Engineering Society.



Xinhui Cui received the B.E. degree in the First Aeronautical Engineering Institute of PLA Air Force, Xinyang, China, in 2005.

He is currently a master graduate at the University of Chongqing, Chongqing, China. His current research interests in micro/nano-transmission platform.



Kai Cheng received the B.E. and M.E. degrees from Harbin Institute of Technology, Harbin, China, in 1983 and 1988, respectively, and the Ph.D. degree from Liverpool John Moores University, Liverpool, UK, in 1993, all in mechanical engineering.

He is currently a Professor at Brunel University, Middlesex, UK. He has authored or coauthored 160 scientific papers. His current research interests in ultra-precision machining and micro-fabrication.

Prof. Cheng is currently a Chair in Manufacturing Systems and Head of AMEE. He is an Editor of the International Journal of Advanced Manufacturing Technology and a member of the Editorial Board of the International Journal of Machine Tools and Manufacture.



Songsong Yu received the B.E. degree in industrial engineering and M.E. degree in mechanical design and theory from Chongqing University, Chongqing, China, in 2004 and 2011, respectively.

He is currently a graduate from the University of Chongqing, Chongqing, China.